24th Cycle of Solar Activity: Geoefficiency of Flares

E. A. Bruevich[a], * and G. V. Yakunina[a], *

[a]*Sternberg State Astronomical Institute, Lomonosov Moscow State University, Moscow, Russia*
*e-mail: red-field@yandex.ru
**e-mail: yakunina@sai.msu.ru

Abstract—Various aspects of the of geoefficiency of solar-activity phenomena, such as flares and coronal mass ejections (CMEs), are considered. The number of geoefficient events was about two times lower in the 24th cycle than in the 23rd cycle. Statistical data on major flares and the *Dst* index in different phases of the 24th cycle is compared. Large flares (X-ray class > M5) were analyzed based on data from GOES-15 satellite observations in the 24th solar activity cycle. The three main geomagnetic indices, *Ap*, *Kp*, and *Dst*, were analyzed in comparison with the $F_{10.7}$ index and the sunspot number (SSN).

INTRODUCTION

Events in solar–terrestrial physics that affect the radiation, geomagnetic, and electromagnetic conditions in the near-Earth space are called geoeffective. Physical processes occurring in the atmosphere of the sun and the heliosphere are the source of such events. The concept of space weather was introduced in 1995 in the United States for a set of phenomena that occur on the Sun or in the solar wind, magnetosphere, or ionosphere and can affect the operation and reliability of satellite- and ground-based technological systems and threaten human health.

The main phenomena of solar activity (SA) that most often cause geoeffective events are flares, coronal mass ejections (CMEs), and high-speed streams (HSSs) of solar wind (SW) from coronal holes (CHs).

The geoeffectiveness of flares is determined by their power (X-ray class) and position on the solar disk. Flares with an X-ray class above M5 that occur in the western half of the solar disk are the most geoeffective.

Another source of geoeffective disturbances are CMEs and HSSs of SW from CHs. According to Gopalswamy et al. (2015, 2018), CMEs and solar flares are physically interconnected in most cases; they occur in the same active region almost simultaneously (within 30 min). Another cause of geomagnetic storms may be the interaction of a high-speed SW from a CH and a low-speed stream. This phenomenon is called a corotating interaction region (CIR). Such interaction results in plasma compression, whereby the density and temperature increase.

According to modern views, geomagnetic storms are caused by disturbed SW streams in the Earth's orbit with the necessary orientation of the interplanetary magnetic field (IMF). During a magnetic storm, there are changes in the horizontal component of the geomagnetic field, which is measured on the Earth's surface at low latitudes; the magnetosphere borders tighten on the day side, and the ring current of energetic particles form in the inner magnetosphere.

The southern component of the magnetic field (*Bz*) and compression make solar and heliospheric disturbances geoeffective. The *Bz* amplifies the southern component of the interplanetary magnetic field, which leads to the reconnection and transfer of SW energy to the magnetosphere. Compression is essential, because it enhances the existing IMF and increases the density. CMEs (as the most geoeffective structures), as a rule, carry long-lasting streams with a strong, southern IMF component. Fast CMEs compress the existing southern IMF with the shock wave, amplifying it.

The frequency of moderate and severe storms on Earth is distinctly related to the 11-year SA cycle. The sources of geomagnetic activity at the maximum and minimum of the solar cycle differ. At the cycle maximum, geoefficiency is associated with large flares and CME. At the cycle minima, the cause of geomagnetic disturbances on Earth is HSSs of SW from CHs.

The SW is a mixture of slow and fast streams. The HSS, in turn, is divided into quasi-stationary and sporadic streams of different natures. Quasi-stationary HSSs of solar plasma, which are responsible for recurrent geomagnetic disturbances, come from CHs. Their speed reaches 700–1000 km/s. Sporadic HSSs are relatively short-lived, complex structures that are responsible for sporadic magnetospheric disturbances, in particular, large magnetic storms. The speed of the sporadic solar streams reaches 1200 km/s; a shock

Table 1. Comparison of active events in the 23rd and 24th cycles

Flares	Number of flares		Events	Number of events	
	23rd cycle	24th cycle		23rd cycle	24th cycle
Flares > M1	1553	755	SPE (>10 МэВ)	90	55
Flares > M5	1408	133	SPE (>10 МэВ) ≥ 1000 pfu	25	8
Flares > X1	125	49	GLE	12	3
Flares > X5	20	5	$Dst \leq -100$ nT	100	27

wave forms at the stream front. Such a shock wave may cause sudden compression of the magnetic field without Dst variation. Significant Dst variation (storm-time variation) requires that the Bz component of the SW magnetic field has a sign opposite to the Earth's magnetic field.

SW HSSs also compress and enhance the southern IMF component in CIRs. This compression is enhanced when a CIR interacts with a CME, which happens mostly during periods far from the maximum solar activity. The SW speed mainly affects compression (Webb et al., 2001).

When a SW HSS from a CH catches up with the slow stream preceding it, the plasma along the interaction line is compressed, which, in turn, leads to an increase in the plasma density and temperature of the slow stream due to the kinetic energy of the fast stream (the CIR region). Reaching the Earth's orbit, CIRs cause geomagnetic storms, but their geoeffectiveness is not very large compared to CMEs. Nevertheless, many researchers attach great importance to the influence of CIRs in connection with the safety of air and space flights.

Thus, the manifestations of solar activity that most often become the cause of geoeffective events near-Earth space environment are solar flares and CMEs.

The goal of the work is to analyze flare activity and its relationship with geomagnetic phenomena, as determined by the indices Kp, Ap, and Dst, and to study the SA manifestations in the 24th cycle.

24th CYCLE OF ACTIVITY. FLARES AS THE PRINCIPAL FACTOR OF SPACE WEATHER

GOES-15 data (http://www.n3kl.org/sun/noaa_archive/) on the large flares (X-ray class > M5) in the 24th SA cycle were analyzed with the use of the World Data Center catalog (http://www.wdcb.ru/stp/data/Solar_Flare_Events/Fl_XXIV.pdf) and data from the National Geophysical Data Center (https://www.ngdc.noaa.gov/stp/solar/sgd.html).

The energetic particles that form in flares and the accompanying CMEs—protons, electrons, nuclei—after interaction with the interplanetary medium can reach the Earth's orbit and have a noticeable effect on space weather.

Upon reaching the Earth's atmosphere, the interplanetary shock wave associated with CMEs, solar proton events (SPEs), and SW HSSs from powerful flares causes magnetospheric storms and substorms. Solar cosmic-ray (SCR) fluxes significantly increase the level of radiation hazard for astronauts and satellite equipment, as well as for aircraft passengers on high-altitude polar routes. In the worst case, powerful SCR fluxes and a large dose of short-wavelength radiation result in the loss of satellites and the failure of the equipment used in space objects. High-energy SCR particles contribute to the formation of nitrogen oxides in the Earth's middle atmosphere, which participate in catalytic cycles of ozone destruction. It is important to take their influence into account in photochemical modeling and in the interpretation of observations at the moments of SPEs or strong geomagnetic disturbances.

The 24th cycle opens the second era of reduced SA (Ishkov, 2018). Figures 1a and 1b show a graph of sunspot numbers (SSNs) averaged by month; the positions of large flares and the change in the Dst index in the 24th cycle are indicated. A total of 170 outbreaks of X-ray class > M5.0 were observed, 58 of which were of class > X1. Note that there was a noticeable asymmetry in flare activity for different hemispheres and different years of the cycle (Bruevich and Yakunina, 2017). According to the Wilcox Solar Observatory (WSO) (http://wso.stanford.edu/), the average background value of the total solar MF has diminished by more than two times (Bruevich and Yakunina, 2015). The decrease in the background values of the total solar MF led to a decrease in geoeffectiveness due to the decrease in the number of geoeffective solar flares, SPEs, and magnetic storms (Table 1).

During the 24th SA cycle, the average magnetic field of sunspots was very low, and the flare activity was also reduced. An important class of proton events is called Ground Level Enhancement (GLE). GLE is recorded with neutron monitors (NMs) (Bazilevskaya et al., 2015). The maximum proton energy measured in this way can reach 15−20 GeV. The strongest flares of the 24th cycle occurred in September 2017 (X.9.4 and X8.3), while there were flares of class X13−X17 in the 23rd cycle. Three geoeffective events were accompanied by GLE in the 24th cycle (one of which was the event of September 10, 2017, Fig. 1b, Table 1) while
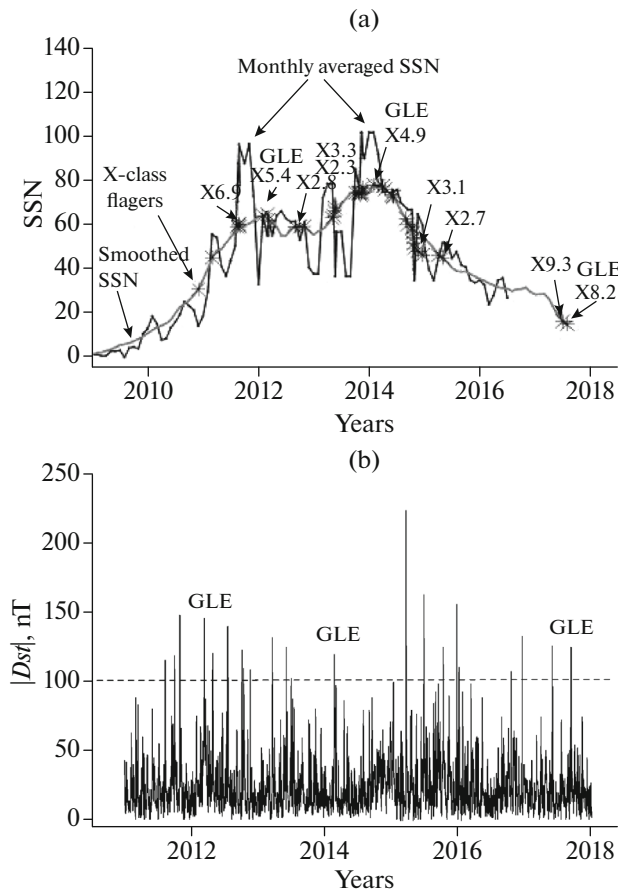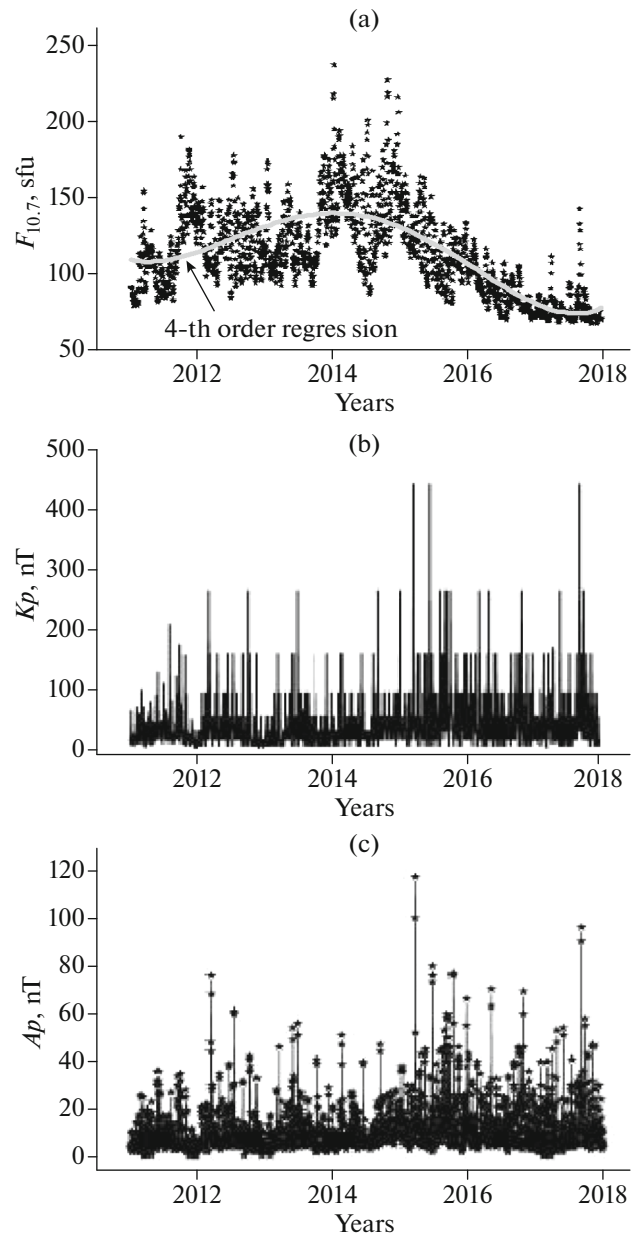
Fig. 1. (a) Variation in the monthly average SSN in the 24th cycle plotted against the largest flares of class X; (b) absolute variations of daily average values of the *Dst* index in the 24th cycle. Note that the maximum number of *Dst* perturbations (b) is shifted relative to the sunspots (a). The strongest *Dst* disturbances occurred in 2015.

Fig. 2. Variation in daily averages: (a) $F_{10.7}$, (b) Kp, and (c) Ap in the 24th cycle. The Kp and Ap indices reach their maximum after the maximum $F_{10.7}$ flux (2014).

there were 12 such events in the 23rd cycle. The GLE deficiency in the 24th cycle apparently reflects a decrease in the number of intense proton fluxes with E > 100 MeV and a decrease in the number of CMEs with velocities exceeding 2000 km/s, which is associated with powerful flares (class > X1).

INDICES OF SOLAR AND GEOMAGNETIC ACTIVITY IN THE 24th CYCLE

Changes in SA are usually characterized by specific indices reflecting geomagnetic disturbances. We studied the indices of geomagnetic activity (Kp, Ap, Dst), which describe the variations in the Earth's magnetic field caused by changes in SA.

Geomagnetic-activity indices are closely related to the solar ones, in particular, to the $F10.7$ index. The $F_{10.7}$ flux is the main SA index; it characterizes the level of solar radiation received by the Earth at a wavelength of 10.7 cm (2800 MHz). The $F_{10.7}$ flux affects

the degree of ionization and electron concentration in the $F2$ ionosphere region. Figure 2a presents the variation in the $F_{10.7}$ flux in the 24th cycle. The 24th is one of the weakest cycles recorded since the middle of the last century.

The Kp is a planetary index of geomagnetic disturbance that characterizes the deviation of the Earth's magnetic field from a calm day curve over a 3-h interval. The Kp scale is quasi-logarithmic; the index was introduced by J. Bartels in 1938. The Kp index is calculated as the average value of Kp indices determined
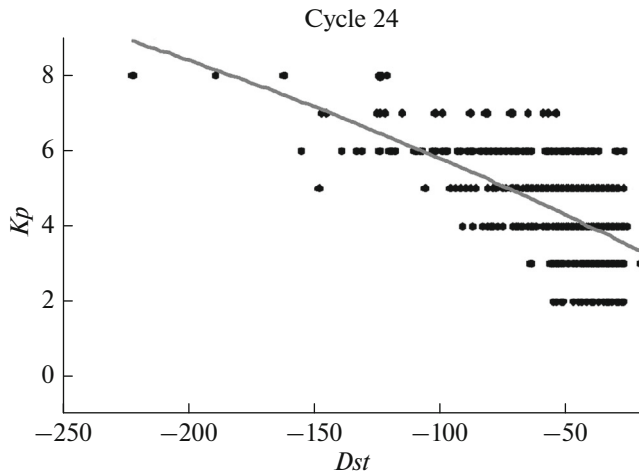
Fig. 3. Ratio of the extreme values of the *Kp* and *Dst* indices for magnetic storms of the 24th cycle.

at 13 geomagnetic observatories at moderate latitudes. Figure 2b presents the changes in the daily values of the *Kp* index in the 24th cycle. There were five cases with $Kp \geq 8$: 17−18.03.2015, $Dst = -222$ nT and -184 nT); 22−23.03.2015 ($Dst = -121$ nT and -184 nT), and 08.09.2017 ($Dst = -121$ nT).

The *Ap* index has often been used of late. The *Ap* index is determined in units of magnetic field, nanotesla (nT); its values vary from 0 to 280 nT. The *Ap* index is the daily average planetary amplitude of the Earth's magnetic field perturbation. Figure 2c presents the variation in the *Ap* index during the 24th cycle.

The *Dst* index of geomagnetic activity at low latitudes was introduced by Sugiura (1964) as a measure of the change in the Earth's magnetic field due to the influence of ring currents arising in the magnetosphere during magnetic storms. On calm days, the *Dst* value lies within ±20 nT; the largest magnetic storms make it reach negative values down to −450 nT. Continuous series of hourly index values are widely used to characterize geomagnetic variations during disturbed and quiet periods (Fig. 1b).

Figure 1a shows the SSN variation and powerful flares in the 24th cycle. Note the characteristic fea-

tures of the 24th cycle, e.g., low SSN values at the maximum, a small number of large flares, and a small number of geoeffective events (Table 1; Ishkov, 2018). The distribution of the *Dst* index in the 24th cycle, which was obtained based on data from the Kyoto World Geomagnetism Data Center (http://wdc.kugi.kyoto-u.ac.jp/dstae/index.html), is shown in Fig. 1b. Note that there were only 27 large geoeffective events with $|Dst| > 100$ nT in the 24th cycle, which were accompanied by powerful magnetic storms. A study of ~100 magnetic storms that occurred from 1996 to 1999 with $Dst \leq -50$ nT or $Kp \geq 5$ (Huttunen et al., 2002) revealed differences in the behavior of the *Dst* and *Kp* indices. A higher number of *Kp* storms were associated with shock waves, while most of *Dst* storms were caused by CMEs. It was discovered that the strongest geomagnetic storms ($Dst \leq -200$ nT, $Kp \geq 8$) were associated with fast CMEs. Almost all most powerful magnetic storms ($Dst \leq -100$ nT, or $Kp \geq 7$) were associated with shock waves and CMEs, although the statistics for moderate storms differed at different phases of the solar cycle.

A method to predict geomagnetic storms with $Dst < -50$ nT was developed by Starodubtsev et al. (2019); the prediction rate of the method was ~70%. Current forecast results are available on the website: http://www.ysn.ru/~starodub/SpaceWeather/global_survey_real_time.html.

Figure 3 shows the ratio of the extreme values of the *Kp* and *Dst* indices for magnetic storms with $-200 < Dst < -60$ nT occurring during the 24th cycle. The nature of the dependence in Fig. 3 corresponds to similar graphs (ambiguous correspondence between the *Kp* and *Dst* indices) for 600 events in cycles 22 and 23 (Ermolaev and Ermolaev, 2006). Note that there were fewer events with $Dst < -100$ nT in the 24th cycle (Table 1).

The distribution of strong ($Kp \geq 5$) magnetic storms in the cycle 24th (Table 2, Fig. 4) is similar to the two-humped distribution of the sunspot number (Fig. 1a).
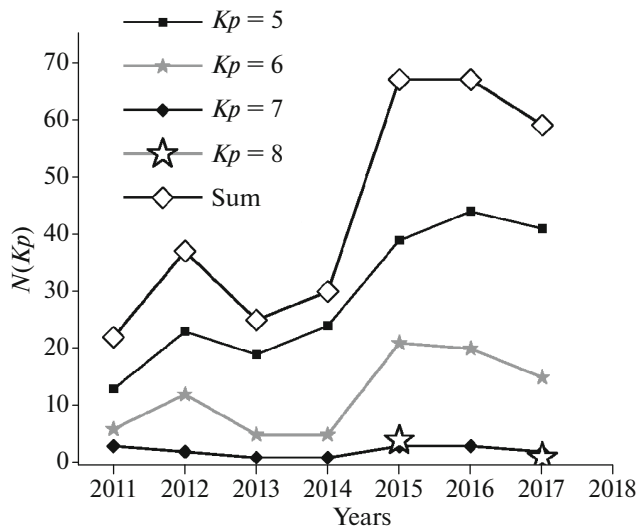
Figure 4 illustrates the average annual distribution of the frequency of the occurrence of *Kp* indices with a given value (>5). It shows that the number of geomagnetic storms sharply increased after 2014. This may be due to the reversal of the magnetic field of the Sun. The increase in the frequency of magnetic storms during the recession phase of the solar cycle can be caused primarily by a SW HSSs from CHs, the number of which reaches a maximum 2−3 years after the maximum of the solar cycle (e.g., Obridko et al., 2013).

3. CONCLUSIONS

The SA manifestations that most often cause geoeffective events in the near-Earth space environment are solar flares and CMEs. Moreover, disturbances in the near-Earth space can be caused by SW HSSs originating from CHs on the Sun surface. Thus, the analysis of flare activity is very important for the assess-

Table 2. Distribution of strong magnetic storms in time

Year	$Kp = 5$	$Kp = 6$	$Kp = 7$	$Kp = 8$	Total
2011	13	6	3		22
2012	23	12	2		37
2013	19	5	1		25
2014	24	5	1		30
2015	39	21	3	4	67
2016	44	20	3		67
2017	41	15	2	1	59

Fig. 4. Distribution of magnetic storms with different Kp indices over the year $N(Kp)$ for the years of the 24th cycle from Table 1.

ment of the situation in the near-Earth space environment during the 24th cycle, as well as for the prediction of geomagnetic activity indices in the near future.

1. Analysis of the observations showed that the 24th cycle is characterized by low flare activity: the number of large flares was about two times lower as compared to cycles 22 and 23. The main contribution to geoeffective events was made by the CMEs accompanying flares.

2. The values of the Kp, Ap, and Dst indices in the 24th cycle are noticeably lower on average than in previous cycles. During the 24th cycle, there was is a sharp increase in the number of geomagnetic storms after 2014.

3. The frequency of the occurrence of moderate and severe storms on Earth is distinctly related to the 11-year cycle of solar activity (Figs. 1a, 1b).

ACKNOWLEDGMENTS

CONFLICT OF INTEREST

The authors declare that they have no conflict of interest.

REFERENCES

Bazilevskaya, G.A., Logachev, Yu.I., Vashenyuk, E.V., et al., Solar proton events in solar activity cycles 21−24, *Bull. Russ. Acad. Sci.: Phys.*, 2015, vol. 79, pp. 573−576.

Bruevich, E.A. and Yakunina, G.V., General trends in the change in solar activity indices in the period from the late XX to early XXI century, *Geomagn. Aeron. (Engl. Transl.)*, 2015, vol. 55, no. 8, pp. 1060−1065.

Bruevich, E.A. and Yakunina, G.V., Flare activity of the Sun and variations in its UV emission during cycle 24, *Astrophysics*, 2017, vol. 60, no. 3, pp. 387−400.

Gopalswamy, N., Mäkelä, P., Akiyama, S., et al., Large solar energetic particle events associated with filament eruptions outside of active regions, *Astrophys. J.*, 2015, vol. 806, no. 1, id 8.

Gopalswamy, N., Mäkelä, P., Akiyama, S., et al., Sun-to-Earth propagation of the 2015 June 21 coronal mass ejection revealed by optical, EUV, and radio observations, *J. Atmos. Sol.-Terr. Phys.*, 2018, vol. 179, pp. 225−238.

Huttunen, K.E.J., Koskinen, H.E.J., and Schwenn, R., Variability of magnetospheric storms driven by different solar wind perturbations, *J. Geophys. Res.*, 2002, vol. 107, *J. Geophys. Res.*, 2002, vol. 107(A7), 1121. https://doi.org/10.1029/2001JA900171

Ishkov, V.N., Space weather and specific features of the development of current solar cycle, *Geomagn. Aeron. (Engl. Transl.)*, 2018, vol. 58, no. 6, pp. 753−767.

Obridko, V.N., Kanonidi, Kh.D., Mitrofanova, T.A., and Shelting, B.D., Solar activity and geomagnetic disturbances, *Geomagn. Aeron. (Engl. Transl.)*, 2013, vol. 53, no. 2, pp. 147−156.

Starodubtsev, S., Baishev, D., Grigoryev, V., et al., Analyzing solar, cosmic, and geophysical events in September 2017 using SHISRA SB RAS complex observations, *Sol.-Terr. Phys.*, 2019, vol. 5, no. 1, pp. 14−27.

Sugiura, M., Hourly values of equatorial Dst for the IGY, *Ann. Int. Geophys. Year*, 1964, vol. 35, pp. 9−45.

Webb, D.F., Crooker, N.U., Plunkett, S.P., et al., The solar sources of geoeffective structures, in *Space Weather (Geophysical Monograph Series)*, American Geophysical Union, 2001, vol. 125, pp. 123−141.

Yermolaev, Yu.I., Yermolaev, M.Yu., Statistical relationships between solar, interplanetary, and geomagnetospheric disturbances, 1976−2000, *Cosmic Res.*, 2006, vol. 40, no. 1, pp. 3−16.

Translated by M. Hannibal